ORIGINAL ARTICLE

Cancer Science WILEY

NAD(P)HX epimerase downregulation promotes tumor progression through ROS/HIF-1α signaling in hepatocellular carcinoma

Bo Sun 🔟 | Lei Yu | Cong Xu 🔟 | Yi-Ming Li | Yan-Rong Zhao | Mo-Mo Cao | Lian-Yue Yang 🔟

Liver Cancer Laboratory, Department of Surgery, Xiangya Hospital, Central South University, Changsha, China

Correspondence
Lian-Yue Yang, Liver Cancer Laboratory, Department of Surgery, Xiangya Hospital, Xiangya Road 87, Changsha 410008, Hunan, China.
Email: lianyueyang@hotmail.com

Funding information
National Natural Science Foundation of China, Grant/Award Number: 81773139; Key Project of National Nature Science Foundation of China, Grant/Award Number: 81330057; National Science & Technology Major Project, Grant/Award Number: 2017ZX10203207-002-003; Specialized Research Fund for Doctoral Program of Higher Education of China, Grant/Award Number: 20130162130007; National Key R&D Program of China, Grant/Award Number: 2016YFC0902400

Abstract

Reactive oxygen species (ROS) derived from aberrant tumor metabolism could contribute to tumor invasion and metastasis. NAD(P)HX Epimerase (NAXE), an epimerase that allows the repair of damaged forms of antioxidant NADPH, is a potential cellular ROS scavenger and its role in tumor development is still elusive. Here, we found that NAXE is significantly downregulated in hepatocellular carcinoma (HCC) tissues and cell lines. NAXE downregulation is associated with poor clinicopathological characteristics and is an independent risk factor for overall and disease-free survival of HCC patients after liver resection. In addition, low NAXE expression could identify worse prognosis of HCC patients before vascular invasion or in early stages of disease. In particularly, low NAXE expression in HCC is markedly associated with microvascular invasion (MVI) and its combination with MVI predicts poorer prognosis of HCC patients after liver resection. Furthermore, in vitro and in vivo experiments both showed that knockdown of NAXE expression in HCC cells promoted migration, invasion, and metastasis by inducing epithelial-mesenchymal transition (EMT), whereas NAXE overexpression causes the opposite effects. Mechanistically, low NAXE expression reduced NADPH levels and further caused ROS level increase and hypoxia-inducible factor-1α (HIF-1α) activation, thereby promoting invasion and metastasis of HCC by facilitating EMT. What is more, the tumor-promoting effect of NAXE knockdown in HCC xenograft can be abolished by giving mice *N*-acetyl-L-cysteine (NAC) in drinking water. Taken together, our findings uncovered a tumor suppressor role for NAXE in HCC by scavenging excessive ROS and inhibiting tumor-promoting signaling pathways, suggesting a new strategy for HCC therapy by targeting redox signaling.

----

1 | INTRODUCTION

Liver cancer is predicted to be the sixth most commonly diagnosed cancer and was the fourth leading cause of cancer death worldwide in 2018 of which HCC accounted for 75%-85% of total cases.[1] Particularly in China, liver cancer was the second leading cause of cancer-related years of life lost.[2] Although various strategies have been explored to prolong life expectancy of HCC patients, postoperative recurrence and metastasis are still major obstacles to improve survival of patients with HCC.[3] Therefore, it is imperative to elucidate new regulatory mechanisms of recurrence and metastasis in HCC and further provide the foundation for targeted therapies.

Reprogrammed metabolism has been deemed an emerging hallmark of cancer.[4] Aberrant metabolism will generate excessive by-products, for example ROS, to promote cancer progression by various mechanisms, including EMT.[5,6] Therefore, scavenging excessive ROS would be an effective way to suppress tumor progression. NADPH is a well known antioxidant that could counteract ROS by maintaining the redox status of glutathione and thioredoxin.[7] However, NADPH is often damaged by enzymatic or heat-dependent hydration during cellular metabolism.[8] In addition, damaged NADPH could inhibit glucose 6-phosphate dehydrogenase, which is a key enzyme for production of NADPH.[9]

By retrieving previous publications, we found that NAD(P)HX Epimerase (NAXE) could act as an epimerase to allow the repair of damaged NADPH, thereby eliminating the toxic effect of metabolic intermediates.[8] Some studies have shown that NAXE gene mutation causes devastating infantile encephalopathy or neurometabolic disorder, indicating the important role of NAXE in oxidative stress conditions.[10-12] NAXE is localized in mitochondria and the cytosol, [13] which is consistent with the major sources of ROS.[14] These facts indicate NAXE may maintain cellular redox balance by participating in the nicotinamide nucleotide repair system. NAXE downregulation is associated with a degree of malignancy in intestinal tumors and could promote colon cancer cell-mediated tumor growth and metastasis.[15] Normal liver has relative high expression and epimerase activity of NAXE,[13,16] but its role in HCC has never been elucidated to date.
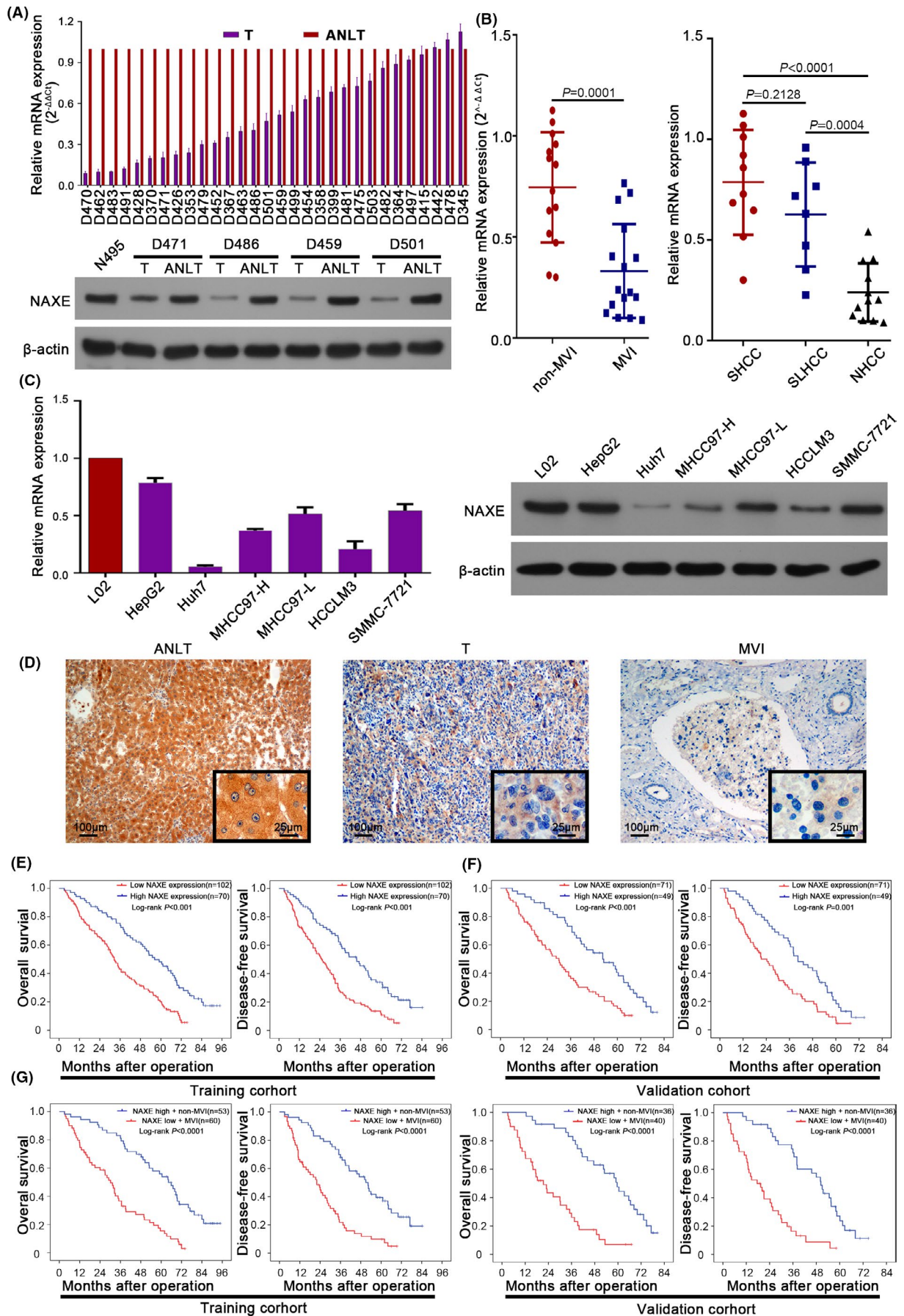
In this study, we found that low NAXE expression predicts poor prognosis of HCC and is closely associated with MVI. Functionally, low NAXE expression promotes HCC invasion and metastasis in vitro and in vivo. Mechanism exploration revealed that NAXE downregulation in HCC could reduce NADPH level and further result in ROS elevation, thereby stabilizing HIF-1α protein and promoting invasion and metastasis by inducing EMT. What is more, NAC could significantly inhibit tumor growth and metastasis in a NAXE knockdown cell derived xenograft.

2 | MATERIAL AND METHODS

2.1 | HCC patients and tissue specimens

In total, 172 specimens were randomly selected from HCC patients who had received curative liver resection at the Department of Surgery, Xiangya Hospital of Central South University from January 2008 to December 2012 and further enrolled into the training cohort (Figure S1A). In addition, another 30 pairs of randomly selected snap-frozen HCC specimens and adjacent nontumorous liver tissues (ANLTs) from this same HCC patient group were used to analysis NAXE mRNA and protein expression. Beyond that, 120 specimens in the validation cohort collected from January 2008 to December 2012 were randomly selected from HCC patients who had received liver resection at Department of Abdominal Surgical Oncology, Affiliated Cancer Hospital of Xiangya School of Medicine, Central South University (Figure S1A). None of enrolled patients had received any preoperative anticancer treatment. All research protocols followed the REporting recommendations for tumor MARKer prognostic studies (REMARK) guidelines for reporting prognostic biomarkers in cancer[17] and was approved by ethics committee of Xiangya Hospital and Affiliated Cancer Hospital of Xiangya School of Medicine at Central South University. Informed consent in writing was obtained from each patient and the study protocol conformed to the ethical guidelines of the 1975 Declaration of Helsinki.

FIGURE 1 NAXE is significantly downregulated in HCC and is a promising prognostic marker for HCC. A, The mRNA and protein expression of NAXE in HCC tissues analyzed by qRT-PCR and western blot. N495 indicates normal liver tissue. B, NAXE mRNA expression in patients with or without MVI and in SHCC, SLHCC and NHCC subgroups. C, The mRNA and protein expression of NAXE in L02 and HCC cell lines analyzed by qRT-PCR and western blot. D, Representative immunohistochemistry images of NAXE in ANLT, HCC, and MVI. The black frames in the lower right corner show a higher magnification of the corresponding images. E and F, Kaplan-Meier analysis (log-rank test) for OS and DFS of HCC patients in training cohort (E) and validation cohort (F) according to NAXE expression level. G, Survival curves of HCC patients in training and validation cohort with high NAXE expression and absence of MVI or with low NAXE expression and presence of MVI. ANLT, adjacent nontumor liver tissue; MVI, microvascular invasion; NHCC, nodular HCC; SHCC, small HCC; SLHCC, solitary large HCC

Clinicopathological variables	Training cohort				Validation cohort			
		NAXE expression				NAXE expression		
	n	Low	High	P-value	n	Low	High	P-value
Gender								
Female	46	25	21		28	13	15	
Male	126	77	49	.424	92	58	34	.117
Age (y)								
≥60	43	27	16		32	18	14	
<60	129	75	54	.591	88	53	35	.695
HBsAg								
Negative	23	11	12		14	5	9	
Positive	149	91	58	.229	106	66	40	.057
Liver cirrhosis								
Absence	52	27	25		40	21	19	
Presence	120	75	45	.195	80	50	30	.293
AFP								
<20 µg/L	67	36	31		44	24	20	
≥20 µg/L	105	66	39	.235	76	47	29	.433
Tumor number								
Solitary	97	49	48		72	34	38	
Multiple	75	53	22	**.008**	48	37	11	**.001**
Tumor size								
≤5 cm	79	39	40		57	28	29	
>5 cm	93	63	30	**.015**	63	43	20	**.033**
Microvascular invasion								
Absence	95	42	53		67	31	36	
Presence	77	60	17	**.000**	53	40	13	**.001**
Macrovascular invasion								
Absence	135	76	59		94	54	40	
Presence	37	26	11	.125	26	17	9	.466
Capsular formation								
Absence	80	57	23		58	42	16	
Presence	92	45	47	**.003**	62	29	33	**.004**
Child-Pugh								
A	110	68	42		79	44	35	
B	62	34	28	.371	41	27	14	.283
Edmondson-Steiner grade								
I-II	96	48	48		64	33	31	
III-IV	76	54	22	**.005**	56	38	18	.070
TNM stage								
I-II	104	53	51		75	38	37	
III-IV	68	49	19	**.006**	45	33	12	**.014**
BCLC stage								
0-A	81	40	41		53	25	28	
B-C	91	62	29	**.012**	67	46	21	**.017**

TABLE 1 The association of NAXE expression with clinicopathological characteristics of HCC in training and validation cohort

Abbreviations: AFP, alpha-fetoprotein; BCLC, Barcelona Clinic Liver Cancer; HBsAg, hepatitis B surface antigen; TNM, tumor node metastasis.

Significant results ($P < .05$) are given in bold.

TABLE 2 Univariate and multivariate analysis of risk factors associated with OS and DFS of HCC patients in training cohort

	OS				DFS			
	Univariate analysis		Multivariate analysis		Univariate analysis		Multivariate analysis	
Variables	HR (95% CI)	*P*-value	HR (95% CI)	*P*-value	HR (95% CI)	*P*-value	HR (95% CI)	*P*-value
Gender								
Female	1				1			
Male	1.296 (0.891-1.884)	.175		NA	1.247 (0.858-1.813)	.247		NA
Age (y)								
<60	1				1			
≥60	1.239 (0.849-1.807)	.266		NA	1.277 (0.881-1.852)	.196		NA
HBsAg								
Negative	1				1			
Positive	1.325 (0.814-2.156)	.257		NA	1.441 (0.865-2.401)	.160		NA
Liver cirrhosis								
Absence	1				1			
Presence	1.352 (0.936-1.953)	.108		NA	1.296 (0.899-1.868)	.166		NA
AFP								
<20 µg/L	1				1			
≥20 µg/L	1.293 (0.915-1.826)	.145		NA	1.339 (0.947-1.893)	.099		NA
Tumor number								
Solitary	1		1		1		1	
Multiple	2.030 (1.443-2.855)	**.000**	1.982 (1.388-2.829)	**.000**	1.793 (1.279-2.514)	**.001**	1.710 (1.198-2.440)	**.003**
Tumor size								
≤5 cm	1				1			
>5 cm	1.333 (0.955-1.863)	.091		NA	1.283 (0.919-1.790)	.143		NA
Microvascular invasion								
Absence	1		1		1		1	
Presence	2.120 (1.509-2.980)	**.000**	1.733 (1.131-2.655)	**.012**	2.074 (1.475-2.915)	**.000**	1.730 (1.130-2.651)	**.012**
Macrovascular invasion								
Absence	1		1		1		1	
Presence	2.180 (1.450-3.276)	**.000**	1.651 (0.975-2.713)	.052	2.053 (1.367-3.082)	**.001**	1.484 (0.901-2.446)	.121
Capsular formation								
Presence	1				1			
Absence	1.282 (0.919-1.789)	.144		NA	1.179 (0.845-1.645)	.332		NA
Child-Pugh								
A	1				1			
B	1.286 (0.910-1.818)	.154		NA	1.239 (0.875-1.754)	.227		NA

(Continues)

TABLE 2 (Continued)

Variables	OS				DFS			
	Univariate analysis		Multivariate analysis		Univariate analysis		Multivariate analysis	
	HR (95% CI)	*P*-value	HR (95% CI)	*P*-value	HR (95% CI)	*P*-value	HR (95% CI)	*P*-value
Edmondson-Steiner grade								
I-II	1		1		1		1	
III-IV	1.726 (1.236-2.411)	**.001**	1.556 (1.086-2.230)	**.016**	1.794 (1.285-2.503)	**.001**	1.639 (1.149-2.338)	**.006**
TNM stage								
I-II	1		1		1		1	
III-IV	1.642 (1.170-2.305)	**.004**	1.934 (1.318-2.837)	**.001**	1.664 (1.188-2.332)	**.003**	1.877 (1.287-2.740)	**.001**
BCLC stage								
0-A	1		1		1		1	
B-C	1.584 (1.129-2.222)	**.008**	1.509 (1.047-2.175)	**.027**	1.615 (1.151-2.265)	**.006**	1.518 (1.054-2.186)	**.025**
NAXE expression								
Low	1		1		1		1	
High	0.444 (0.309-0.637)	**.000**	0.605 (0.395-0.926)	**.021**	0.466 (0.328-0.664)	**.000**	0.640 (0.421-0.971)	**.036**

Abbreviations: AFP, alpha-fetoprotein; BCLC, Barcelona Clinic Liver Cancer; CI, confidence interval; HBsAg, hepatitis B surface antigen; HR, hazard ratio; NA, not applicable; TNM, tumor node metastasis.

Significant results ($P < .05$) are given in bold.

2.2 | Statistical analysis

Statistical analyses were performed using Statistical Product and Service Solutions (SPSS) version 20.0 (IBM) and GraphPad Prism 6 (GraphPad Software). Data were presented as the mean ± standard deviation (SD) from at least 3 independent experiments. The differences of quantitative data were compared using Student *t* test for 2 groups or by one-way ANOVA for more than 2 groups. Categorical data were analyzed by the χ^2 test or Fisher exact test. Correlations between different protein expression levels were analyzed using Spearman's rank analysis. Survival curves were constructed using the Kaplan-Meier method and evaluated using the log-rank test. Univariate and multivariate analysis were analyzed by Cox proportional hazard regression model to identify independent risk factors. All tests were 2-tailed and a *P*-value of < .05 was considered as statistically significant. A complete description of the methods is available in Supporting Material and Methods.

3 | RESULTS

3.1 | NAXE is significantly downregulated in HCC tissues and cell lines

mRNA and protein expression of NAXE was frequently downregulated in HCC tissues compared with ANLTs (Figure 1A). HCC without MVI had higher NAXE expression than that with MVI (Figure 1B). Similarly, HCC tissues without MVI or with MVI had significantly low expression of NAXE than ANLTs (Figure S1B). Our previous researches had found and defined a specific HCC subtype named SLHCC with relatively favorable prognosis similar to small HCC (SHCC).[18] Further studies showed that the gene expression profile of SLHCC was different to nodular HCC (NHCC) with poor prognosis.[19,20] NAXE expression in SLHCC and SHCC is markedly higher than in NHCC, but there was no significant difference between SLHCC and SHCC (Figure 1B). Further analysis

FIGURE 2 Low NAXE expression promotes proliferation, migration, and invasion of HCC in vitro and in vivo. A and B, Effects of NAXE knockdown and overexpression on cell proliferation rate (A) and colony formation capacity (B). The data are quantified in Figure S3C. *$P < .05$; **$P < .01$. C, Wound healing and transwell invasion assays are performed to detect migratory and invasive ability of indicated cells. The data are quantified in Figure S3D,E. D and E, Subcutaneous tumors (D) and orthotopic tumors (E) from HepG2^{shNAXE}, Huh7^{NAXE}, and their control cells are shown in the upper and lower 2 panels respectively. Tumors size is measured 3 times and compared in the right bar graphs with mean ± SD. F, Representative images of mice intrahepatic metastatic nodules and lung tissue sections in each group. Incidence rate (the number of mice with intrahepatic or pulmonary metastasis/total number of mice used in each group, n = 5) of intrahepatic or lung metastasis in each group is shown in the right bar graphs
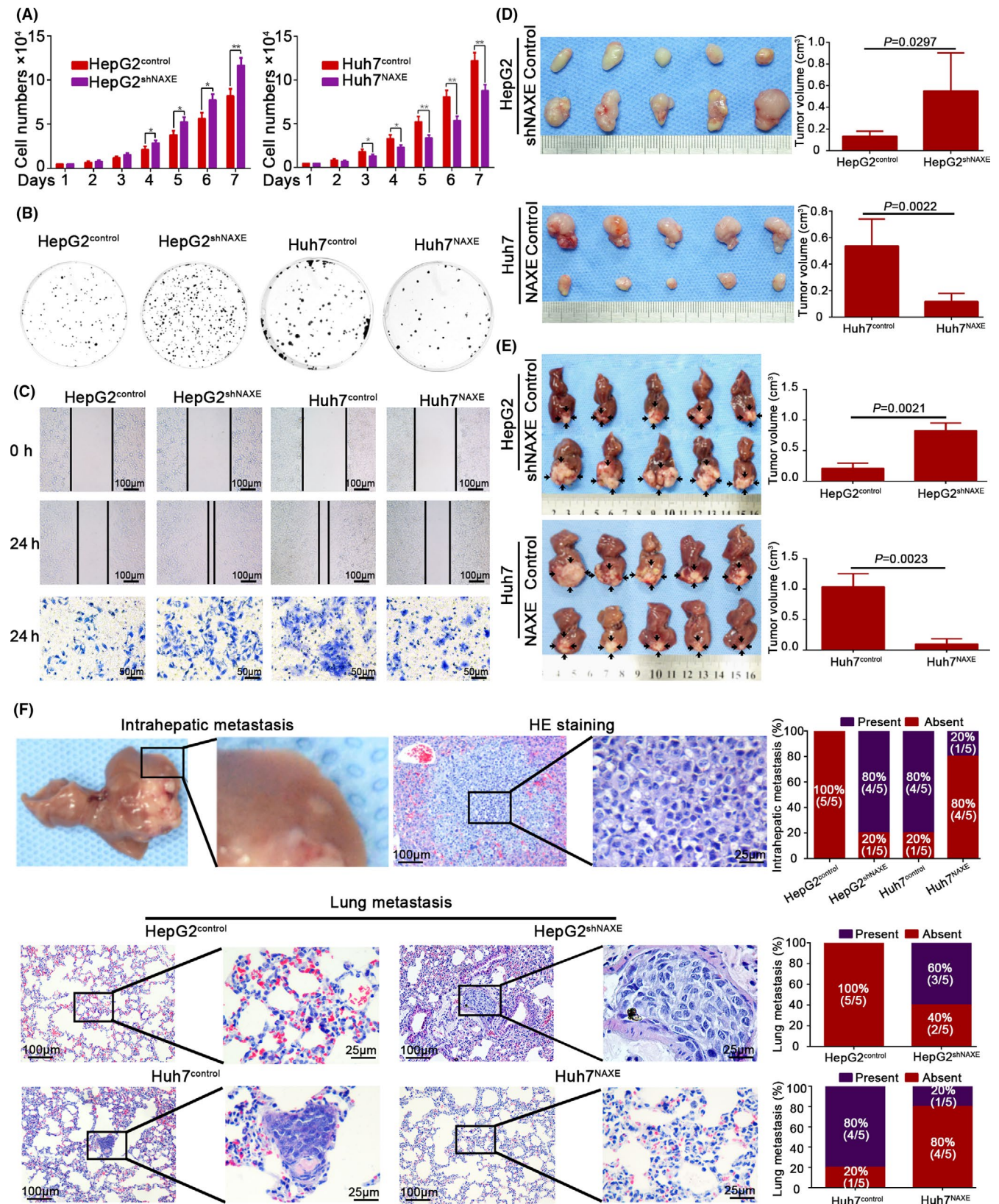
showed there was no significant difference between ANLTs and SHCC, but NAXE was significantly lower in SLHCC and NHCC compared with ANLTs (Figure S1C). NAXE expression of early HCC and advanced HCC was significantly lower than ANLTs (Figure S1D).

Moreover, we could also observe that NAXE downregulation was more obvious in HCC with MVI, advanced HCC, and NHCC. All HCC cell lines had lower NAXE expression than L02, an immortalized human normal liver cell line. Lowly invasive and metastatic
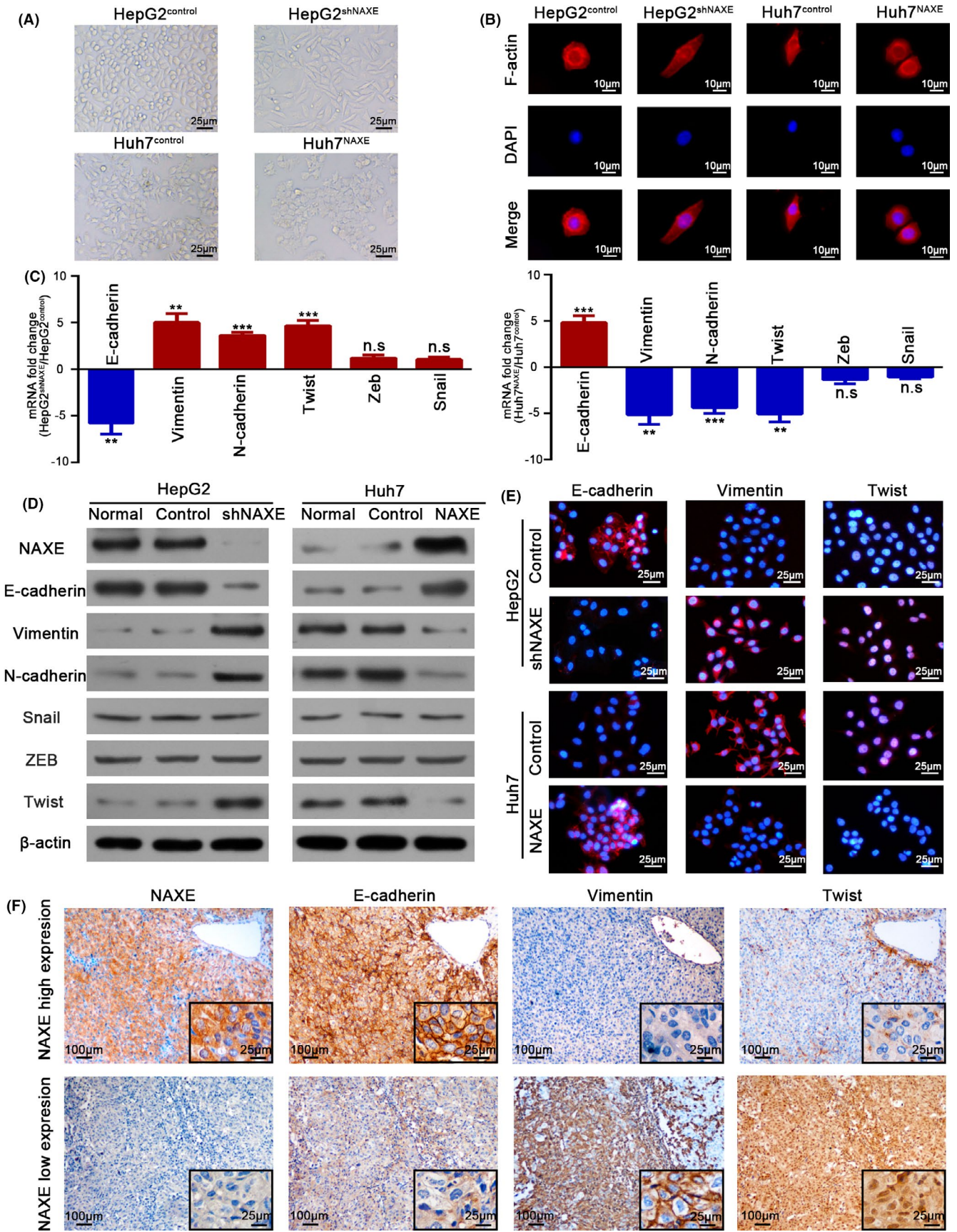
FIGURE 3 Low NAXE expression promotes EMT in HCC. A, Representative cellular morphology of HepG2^{shNAXE}, Huh7^{NAXE}, and their control cells. B, Cytoskeleton of indicated cells is visualized by staining F-actin with rhodamine-phalloidin. DAPI was used to stain nuclei. C, Fold change of mRNA expression for epithelial and mesenchymal markers, as well as EMT-associated transcription factors is compared in NAXE-interfered HCC cells. **$P < .01$; ***$P < .001$; n.s., no significant difference. D, Protein expression of epithelial and mesenchymal markers, as well as EMT-associated transcription factors is detected by western blot. E, Representative immunofluorescence images of E-cadherin, vimentin, and Twist in indicated cells. The nuclei are stained by DAPI. F, Serial sections of HCC tissues with high or low NAXE expression are immunostained to detect E-cadherin, vimentin and Twist expression. The black frames in the lower right corner show higher magnification of corresponding images

HepG2 and SMMC-7721 cell lines had higher NAXE expression than highly invasive and metastatic Huh7 and HCCLM3 cell lines (Figure 1C).[21-24] In cancer, CpG island hypermethylation in promoter regions could lead to silencing of tumor suppressor genes.[25] Therefore, we speculated that downregulation of NAXE in HCC may be associated with CpG island methylation. Interestingly, we found there was a CpG island in the promoter region of the *NAXE* gene (Figure S1E). Further results showed that the methylation level of HCC tumor tissues was significantly higher than that of the corresponding ANLTs (Figure S1F), which indicated that CpG island hypermethylation may be the cause for NAXE downregulation in HCC. IHC staining showed that NAXE protein expression decreased progressively from ANLT, tumor tissue, to MVI (Figure 1D). These data proved that NAXE expression in HCC was frequently suppressed, suggesting that its downregulation may play a certain role in HCC development.

3.2 | Low NAXE expression correlates with poor clinicopathological characteristics and predicts poor prognosis of HCC patients

We then asked whether NAXE downregulation in HCC was associated with poor clinicopathological features and prognosis of HCC patients. There were no significant differences in baseline characteristics among the 2 cohorts (Table S1). In the training cohort, NAXE expression was significantly lower in HCC patients with larger tumor size ($P = .015$), multiple tumor numbers ($P = .008$), MVI ($P < .001$), no capsular formation ($P = .003$), higher pathological grade ($P = .005$), advanced TNM stage ($P = .006$), and Barcelona Clinic Liver Cancer Stage (BCLC) ($P = .012$) (Table 1). Moreover, patients in the low NAXE expression group had significantly shorter OS and DFS than those in the high NAXE expression group from the training cohort (Figure 1E). Univariate and multivariate analysis revealed that low NAXE expression was an independent risk factor for both OS and DFS in the training cohort (Table 2). Similar conclusions were further verified in the validation cohort (Figure 1F; Tables 1 and S2). Then, we further analyzed the prognosis of specific subgroups of HCC patients stratified according to MVI, macrovascular invasion, and BCLC stage. The results in the training and overall cohorts showed that low NAXE expression could discriminate patients with a poor prognosis before the presence of MVI, macrovascular invasion, or in the early BCLC stage (Figure S2A-C). What is more, patients with low NAXE expression and MVI had a statistically more significant reduction in OS and

DFS in the training and validation cohorts compared with those with high NAXE expression and non-MVI (Figure 1G). These data confirmed that low NAXE expression was a worthy prognostic biomarker for HCC patients after liver resection.

3.3 | Low NAXE expression promotes HCC proliferation, migration, and invasiveness in vitro

To further understand the biological function of NAXE in HCC, NAXE expression in HepG2 cells was silenced using shRNA and in Huh7 cells with endogenous lower NAXE expression NAXE was stably overexpressed. NAXE expression levels in these cell lines was tested using qRT-PCR and western blotting (Figure S3A,B). The proliferation rate for HepG2^{shNAXE} was significantly faster than for HepG2^{control} (Figure 2A) and, as expected, colonies derived from HepG2^{shNAXE} were also significantly more numerous than in from control cells (Figure 2B and quantified in Figure S3C). In contrast, proliferation rate and colony formation capacity of Huh7^{NAXE} were clearly suppressed (Figure 2A,B and quantified in Figure S3C). In addition, NAXE downregulation in HepG2 potently promoted wound closure and transwell invasive capacity, whereas NAXE overexpression in Huh7 significantly inhibited its intrinsic highly migratory and invasive capacity (Figure 2C and quantified in Figure S3D,E). All of these results revealed that low NAXE expression could promote HCC cell proliferation, migration, and invasion in vitro.

3.4 | Low NAXE expression facilitates HCC progression in vivo

We then examined whether low NAXE expression could promote HCC growth and metastasis in vivo by mouse subcutaneous and orthotopic xenograft model. First, NAXE expression levels in xenograft tumors were examined by IHC (Figure S4A). The final volume of subcutaneous tumors formed by HepG2^{shNAXE} was significantly larger than that formed by HepG2^{control}. In contrast, Huh7^{NAXE}-derived xenografts had markedly smaller tumor sizes than the Huh7^{control}-derived xenografts (Figure 2D). Consistently, the liver orthotopic xenograft model also revealed similar results, corresponding to subcutaneous tumors (Figure 2E). H&E staining of the orthotopic tumor boundary showed that HepG2^{shNAXE}-derived and Huh7^{control}-derived tumors had a more invasive edge than tumors derived from HepG2^{control} and Huh7^{NAXE}, respectively (Figure S4B). We further
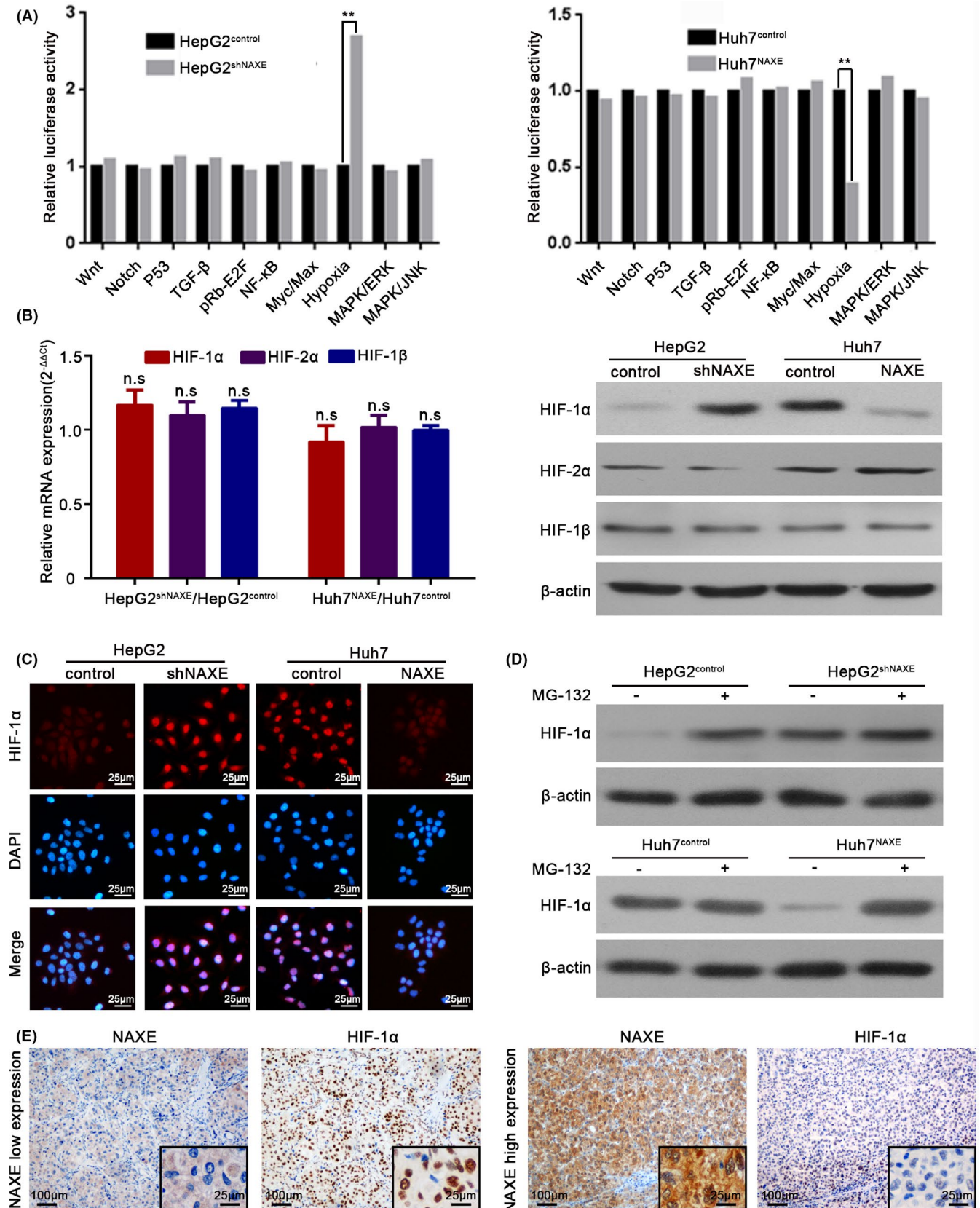
assessed the role of NAXE in HCC metastasis in vivo by serial sectioning of liver and lung. Figure 2F shows representative images of intrahepatic metastasis nodules and pulmonary metastasis for each

group. As was indicated, NAXE overexpression could reduce intrahepatic and pulmonary metastasis, whereas NAXE downregulation could promote HCC metastasis. Together, these results revealed

FIGURE 4 NAXE inhibits HIF-1α signaling by promoting proteasomal degradation in HCC. A, Crucial tumor-associated signaling pathways influenced by NAXE are analyzed by Cignal Finder Cancer 10-Pathway Reporter Array in NAXE-interfered cell lines. **P <.01. B, mRNA fold change and protein expression of 3 HIF subunits are analyzed by qRT-PCR and western blot respectively. n.s., no significant difference. C, Immunofluorescence analysis of HIF-1α protein and its subcellular localization in HepG2^shNAXE^, Huh7^NAXE^, and their control cells. DAPI was used to stain nuclei. D, Western blots for HIF-1α with the lysate of HepG2^shNAXE^, Huh7^NAXE^, and their control cells after treated with the presence or absence of MG-132 (10 μmol/L) for 6 h. E, Representative immunohistochemistry images of NAXE and HIF-1α using serial HCC sections

that NAXE could inhibit HCC growth and dampen distant metastasis in vivo.

3.5 | Downregulation of NAXE expression induces EMT in HCC

Compared with the oval shape of HepG2^control^ cells, we found that HepG2^shNAXE^ exhibited a spindle-like appearance. In contrast, the Huh7^control^ with fibroblastic-like morphology transformed to a typical epithelial phenotype after overexpressing NAXE (Figure 3A). In addition, fluorescence of cytoskeleton revealed that HepG2^shNAXE^ displayed a threadlike F-actin filament compared with the HepG2^control^, whereas Huh7^NAXE^ presented a circular and shrinkable F-actin fiber compared with Huh7^control^ (Figure 3B). To our knowledge, the morphological hallmark of EMT is that the cobblestone appearance of epithelial cells transforms to a mesenchymal cell fusiform shape. EMT is an important biological process not only in critical phases of embryogenesis but also in tumor formation and evolution.[26,27] Knockdown of NAXE expression in HepG2 dramatically downregulated mRNA and protein levels of the epithelial marker E-cadherin, whereas mesenchymal markers, such as vimentin and N-cadherin, were significantly upregulated. In addition, only Twist expression, but not other 2 classical EMT-associated transcription factors, Snail and ZEB, was increased after inhibiting NAXE expression in HepG2. In contrast, NAXE overexpression in Huh7 cells induced the opposite results (Figure 3C-E). What is more, IHC for HCC serial sections showed that NAXE expression positively correlated with E-cadherin expression and negatively correlated with vimentin and Twist expression (Figures 3F and S5A,B). These results suggested that downregulation of NAXE could promote HCC progression by inducing EMT.

3.6 | NAXE inhibits HIF-1α signaling by promoting proteasomal degradation in HCC

To gain insights into the molecular mechanisms by which NAXE inhibit HCC progression, we adopted a Cignal Finder Cancer 10-Pathway Reporter Array and results indicated that NAXE could dramatically attenuate hypoxia signaling (Figure 4A). The core regulators of the hypoxia signaling pathway were hypoxia-inducible factors, which included 2 major alpha subunits (HIF-1α and HIF-2α) and one common beta subunit (HIF-1β). Active HIFs are heterodimeric transcription factors that contain one alpha subunit and one beta subunit.[28,29] Interestingly, knockdown or overexpression of NAXE

caused no altered in mRNA expression of 3 subunits, whereas HIF-1α protein, but not HIF-2α and HIF-1β protein, was significantly altered (Figure 4B). The inhibition of HIF-1α protein expression by NAXE was further confirmed by IF analysis (Figure 4C). Next, we detected the HIF-1α protein levels in either the presence or absence of proteasome inhibitor MG132. MG132 significantly increased HIF-1α protein levels in HepG2^control^ and Huh7^NAXE^ and these were even higher in HepG2^shNAXE^ and Huh7^control^ (Figure 4D). What is more, through IF analysis, we found that undegraded cytoplasmic HIF-1α protein in NAXE knocked-down cells was translocated to the nucleus, this was further confirmed by western blot using cytoplasmic and nuclear fractions (Figure S6A). Next, we overexpressed a HIF-1α mutant with constitutive activation even in aerobic atmosphere in HepG2 cells[30] and depleted endogenous expression of HIF-1α in Huh7 cells using shRNA (Figure S6B). However, manipulation of HIF-1α expression in both 2 cell lines caused no altered NAXE expression, indicating that HIF-1α existed downstream of NAXE (Figure S6C). IHC for clinical specimens of HCC also revealed a negative correlation between NAXE and HIF-1α (Figures 4E and S6D). HIF-1α is well known angiogenic transcription factor that induces the expression of vascular endothelial growth factor (VEGF).[31] Here, qRT-PCR and western blot results showed that the knockdown of NAXE in HepG2 cells increased VEGF expression, while NAXE overexpression in Huh7 cells decreased its expression (Figure S6E). In addition, the tube formation ability of HUVEC was increased after culture in conditioned medium obtained from HepG2^shANXE^ cells and was decreased after using conditioned medium from Huh7^NAXE^ cells (Figure S6F). These results strongly suggested that downregulation of NAXE could activate HIF-1α signaling in HCC.

3.7 | Activated HIF-1α signaling is associated with NAXE downregulation-induced HCC migration, invasion, and EMT

Much evidence has shown that HIF-1α plays a critical role in mediating tumor progression, including the EMT process.[32] We next questioned whether HIF-1α signaling was instrumental in low NAXE induced HCC progression. We first transfected HepG2^shNAXE^ with HIF-1α shRNA lentivirus and overexpressed the above-mentioned HIF-1α mutant in Huh7^NAXE^ cells (Figure S7A). Interestingly, NAXE knockdown-induced cell migration and invasion in HepG2 cells could be re-inhibited by HIF-1α downregulation (Figure 5A; quantified in Figure S7B). What is more, NAXE downregulation caused a mesenchymal phenotype in HepG2 cells that could also be reversed by depletion of HIF-1α (Figure 5B,C). Consistently, upregulated HIF-1α
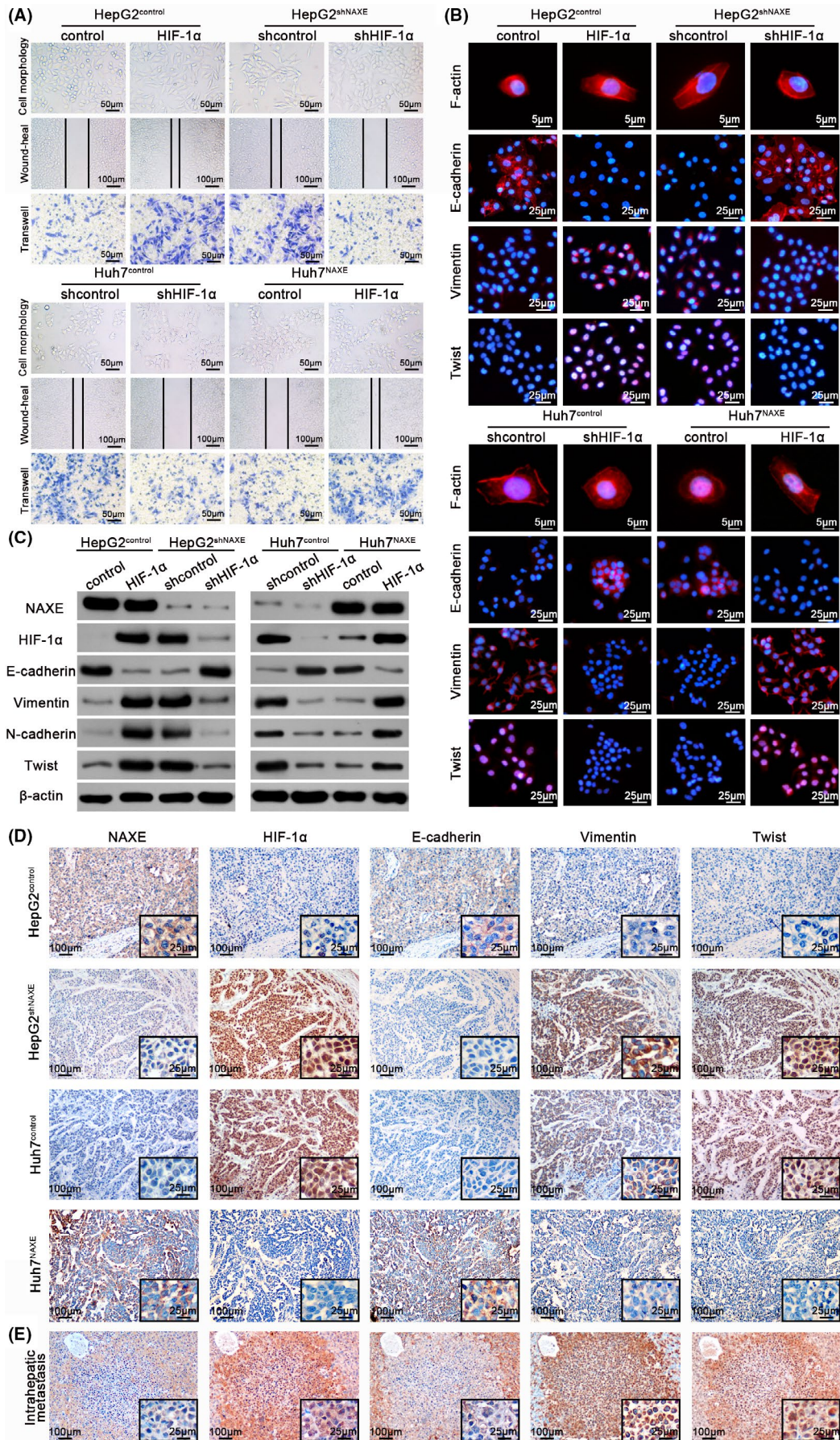
FIGURE 5 Low NAXE expression promotes HCC migration, invasion, and EMT by activating HIF-1α signaling. A, Representative images of cytomorphology, migration and invasion assay for NAXE-interfered cells and control cells with HIF-1α expression inhibited or restored. The data are quantified in Figure S7B,C. B, Fluorescence images of cytoskeleton, E-cadherin, vimentin, and Twist for indicated cells with either HIF-1α re-inhibited or re-introduced. Nuclei are identified by DAPI. C, The protein expression of EMT markers and Twist in indicated cells with either HIF-1α re-inhibited or re-introduced. D and E, Representative immunohistochemistry images of indicated molecules using consecutive sections of liver orthotopic tumors (D) and intrahepatic metastatic nodule (E). The black frames in the lower right corner show higher magnification of corresponding images

mutant in HepG2^control cells significantly promoted its migration, invasion, and EMT process (Figure 5A-C; quantified in Figure S7B). In contrast, suppressed migration and invasion capacity and epithelial features induced by NAXE overexpression in Huh7 cells were recovered by ectopic expression of the HIF-1α mutant (Figure 5A-C; quantified in Figure S7C). In addition, we also knocked down HIF-2α in HepG2^shNAXE cells. Wound healing assay (Figure S7D), transwell assay (Figure S7E) and western blot (Figure S7F) all showed that knockdown of HIF-2α could not reverse the increased migratory, invasive ability and EMT of HepG2^shNAXE cells, indicating that HIF-2α was not the downstream key effector protein of NAXE. Furthermore, IHC analysis for consecutive sections of mouse liver orthotopic tumors showed that tumors with high NAXE expression exhibited high expression of E-cadherin and low expression of HIF-1α, vimentin, and Twist, whereas reverse relationships were observed in low NAXE expression xenografts (Figure 5D). What is more, IHC for intrahepatic metastatic nodules derived from low NAXE expression tumors also showed these relationships (Figure 5E). These results proved that HIF-1α plays an important role in mediating NAXE downregulation-induced HCC migration, invasion, and EMT.

3.8 | NAXE inhibits HIF-1α signaling by eliminating ROS in HCC

The fact that hypoxia environment could stabilize HIF-1α protein had been widely accepted.[33] However, in this study, we found that NAXE downregulation could stabilize HIF-1α in a normoxic environment. Previous studies have reported that ROS could stabilize HIF-1α in normoxia[34,35] and we had inferred that low NAXE expression may cause cellular oxidative stress, leading us to ask whether ROS was critical for NAXE downregulation-mediated HIF-1α stabilization. Therefore, we first tested ROS levels in HepG2^shNAXE, Huh7^NAXE, and their control cells by using 2,7-dichlorofluorescin diacetate (DCFH-DA). Indeed, downregulation of NAXE in HepG2 cells increased ROS levels, whereas overexpression of NAXE in Huh7 cells significantly reduced ROS levels (Figure 6A). Contrary to the changes in ROS levels, NADPH levels decreased after downregulating NAXE expression in HepG2 and increased after upregulating NAXE expression in Huh7 (Figure S8A, left panel). Moreover, the ratio of damaged NADPH/total NADPH was increased in HepG2^shNAXE cells compared with control cells, while this ratio was decreased after overexpressing NAXE in Huh7 cells (Figure S8B, right panel). Interestingly, HIF-1α protein levels in HepG2^shNAXE returned to the levels of the control cells after treatment with NAC, a well known antioxidant used to scavenge ROS[36] (Figure 6B). Additionally, treating Huh7^NAXE

with H_2O_2 restored HIF-1α protein expression dramatically. As expected, increasing ROS levels in HepG2 control cells or decreasing ROS levels in Huh7 cells also increased or decreased HIF-1α protein levels. However, mRNA expression of HIF-1α was not altered after treatment with NAC or H_2O_2 (Figure 6B). Eliminating ROS by NAC in HepG2^shNAXE promoted epithelial transformation and reversed its increased wound healing and transwell capacity. Furthermore, treatment of HepG2^control with H_2O_2 alone induced EMT and increased its migration and invasion ability. (Figures 6B-D and S8B, and quantified in Figure S8C) In contrast, adding H_2O_2 into Huh7^NAXE or NAC into Huh7^control caused the opposite effects (Figures 6B-D and S8B, and quantified in Figure S8D). Finally, to explore potential intervention measures for NAXE downregulation, we used NAC treatment by adding NAC into the mouse drinking water. The results showed that NAC could significantly inhibit tumor growth (Figure 6E) and metastasis (Figure 6F) of orthotopic tumors derived from HepG2^shNAXE and Huh7^control cells with low NAXE expression, indicating that NAC may be a potential therapy to reverse poor outcomes of NAXE downregulation in HCC. Taken together, these data supported the idea that low NAXE expression decreased NADPH levels and further contributed to ROS increase, thereby allowing HIF-1α stabilization and activating its transcriptional activity to promote HCC invasion and metastasis (Figure 7).

4 | DISCUSSION

Apolipoprotein A-I-Binding Protein (AIBP) was first identified in screening proteins that interacted with apolipoprotein A-I (apoA-I).[16] Further research revealed that AIBP could accelerate cholesterol efflux from endothelial cells or macrophages to inhibit angiogenesis, instruct hematopoietic stem cells, or reduce atherosclerosis.[37-39] However, Marbaix et al demonstrated that AIBP, which distributes in mitochondria and cytosol but is not secreted to extracellular space, could catalyze epimerization of R to S forms of NADPHX to repair damaged nicotinamide nucleotides.[8,13] The *AIBP* gene was now renamed *NAXE* by the Human Genome Organisation (HUGO) Gene Nomenclature Committee, which has caused controversy about its function.[40] NAXE expression is relatively high in normal liver and the HCC cell line HepG2 and liver possesses high activity for both cholesterol metabolism and NADPHX epimerase.[16] Previous study have revealed that, in HepG2, NAXE is mainly localized intracellularly with low levels secreted from cells and that its secretion follows a constitutive pattern unaffected by incubation with apoA-I or high-density lipoprotein (HDL).[16] Indeed, our results also showed high NAXE expression in normal liver, ANLT, and L02 cells, and its
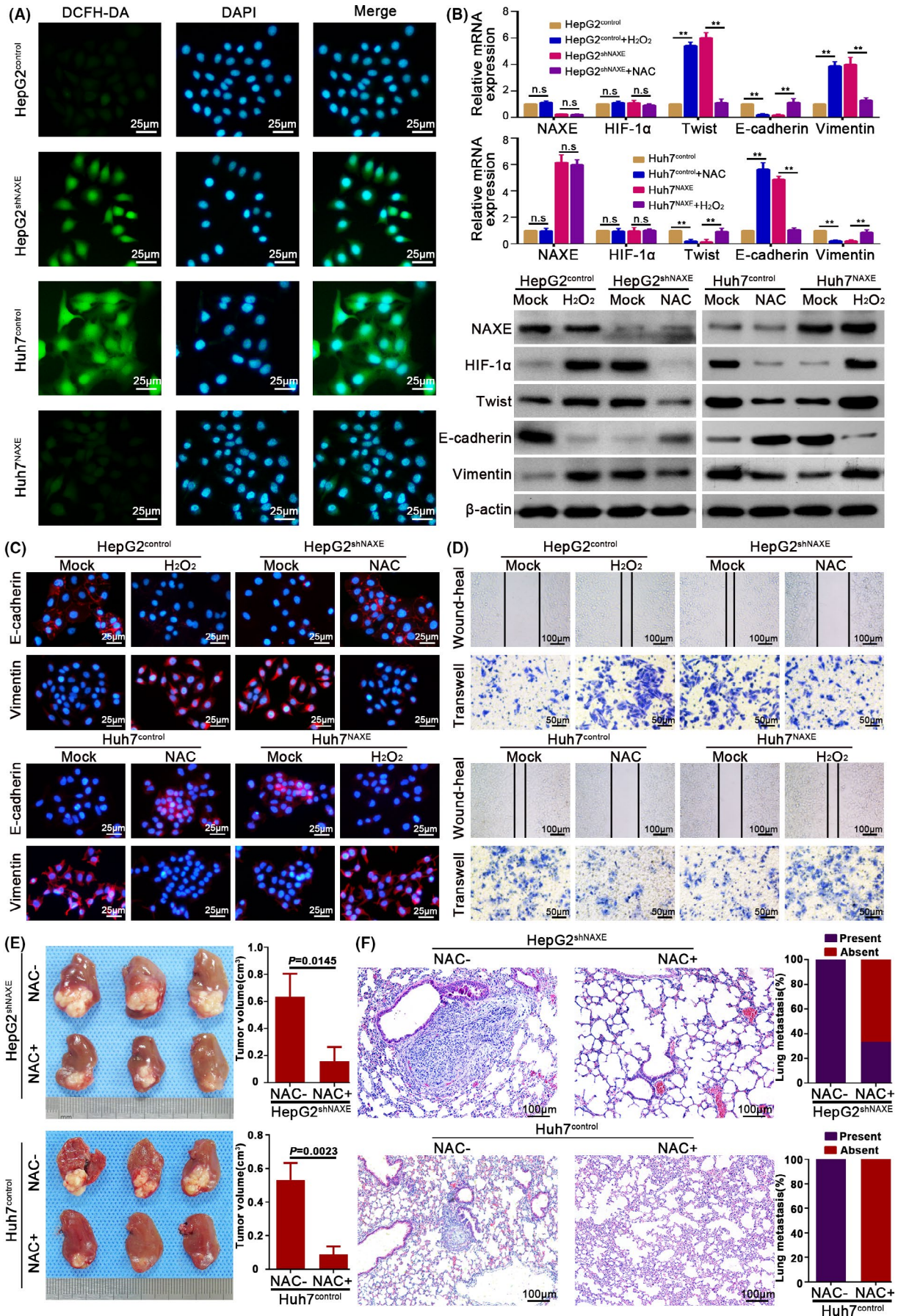
(A) DCFH-DA, DAPI, Merge columns for HepG2control, HepG2shNAXE, Huh7control, Huh7NAXE

(B) Relative mRNA expression bar graphs (HepG2control, HepG2control+H2O2, HepG2shNAXE, HepG2shNAXE+NAC; Huh7control, Huh7control+NAC, Huh7NAXE, Huh7NAXE+H2O2) for NAXE, HIF-1α, Twist, E-cadherin, Vimentin; western blots for NAXE, HIF-1α, Twist, E-cadherin, Vimentin, β-actin

(C) E-cadherin and Vimentin immunofluorescence for HepG2control (Mock, H2O2), HepG2shNAXE (Mock, NAC), Huh7control (Mock, NAC), Huh7NAXE (Mock, H2O2)

(D) Wound-heal and Transwell assays for HepG2control (Mock, H2O2), HepG2shNAXE (Mock, NAC), Huh7control (Mock, NAC), Huh7NAXE (Mock, H2O2)

(E) Tumor images and tumor volume graphs for HepG2shNAXE (NAC-, NAC+; P=0.0145) and Huh7control (NAC-, NAC+; P=0.0023)

(F) Lung histology and lung metastasis (%) for HepG2shNAXE (NAC-, NAC+) and Huh7control (NAC-, NAC+)

FIGURE 6 NAXE inhibits HIF-1α signaling by eliminating ROS in HCC. A, Representative images show ROS level in indicated cells. DCFH-DA is used as a probe to detect ROS level. The nuclei are stained by DAPI. B, mRNA and protein expression of indicated molecules in HepG2^{shNAXE}, Huh7^{NAXE}, and their control cells with either presence or absence of NAC (10 mmol/L) or H_2O_2 (5 μmol/L) treatment. **$P < .01$. C, IF analysis shows expression of E-cadherin and vimentin in NAXE-interfered cells and their control cells after treated with H_2O_2 (5 μmol/L) or NAC (10 mmol/L) or mock treatment. D, Wound-heal and transwell assays respectively show the influence of H_2O_2 (5 μmol/L) or NAC (10 mmol/L) on migration and invasion capacity of HepG2^{shNAXE}, Huh7^{NAXE}, and their control cells. The data are quantified in Figure S8C,D. E, Mice bearing orthotopic tumors derived from HepG2^{shNAXE} and Huh7^{control} cells are treated with NAC by adding into drinking water (supplement with 40 mmol/L NAC for the entire duration of experiment), which could reverse HCC growth and metastasis caused by NAXE downregulation. F, Representative mice lung tissue sections from HepG2^{shNAXE} and Huh7^{control} cells treated with or without NAC. The incidence rate of lung metastasis is shown in right bar graphs
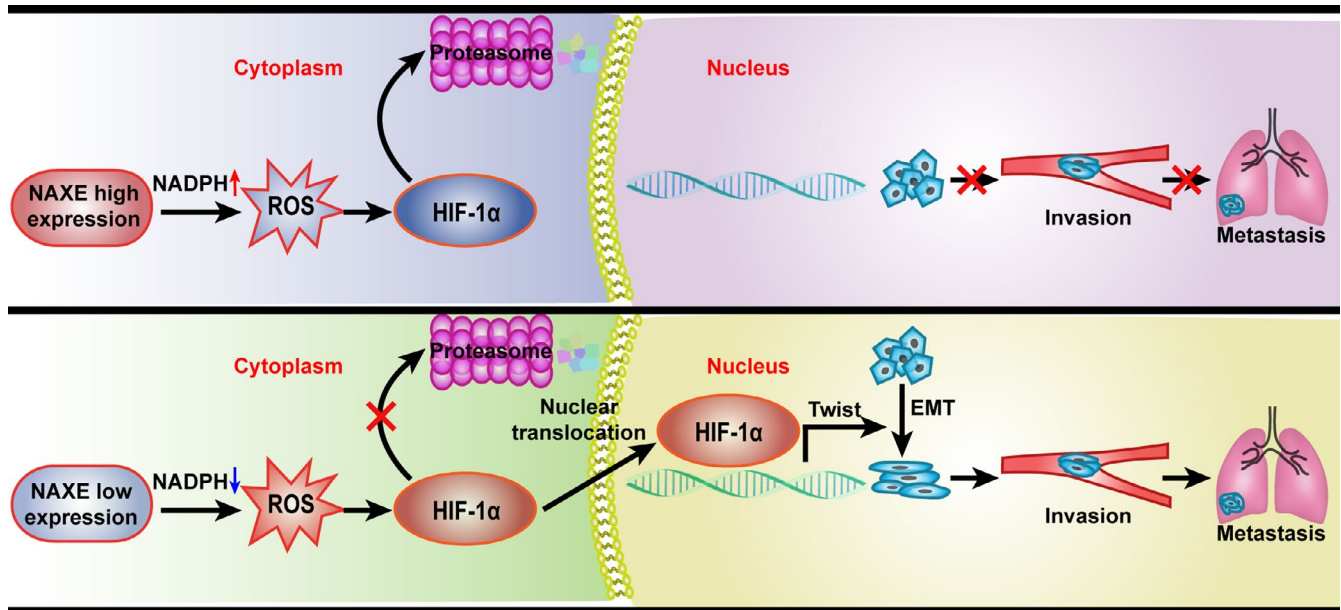

FIGURE 7 Graphical table of contents. The schematic diagram indicates NAXE downregulation in HCC stabilizes HIF-1α and facilitates it nuclear translocation by elevating ROS level. The consequent activation of EMT process further promotes invasion and metastasis of HCC

subcellular distribution revealed by IHC was mainly localized in the cytoplasm. These facts indicated that the function of NAXE in liver was mainly localized in the cytoplasm. The discrepancy of this present study with previous findings could be explained reasonably by the fact that, contrary to endothelial cells or macrophages using HDL to promote cholesterol efflux, liver is an organ mainly involved in HDL cholesterol intake and biliary secretion.[41] Conversely, these results may also suggest that there is distinct role for NAXE in different tissues or organs.

NAXE expression was downregulated in HCC and low NAXE expression was associated with poor clinicopathological characteristics and was also an independent risk factor for both OS and DFS. In the early stages of disease, patients with HCC with a relatively favorable prognosis could be further stratified into 2 groups with significantly different prognoses, which would be useful for clinical decision making. The analysis between subgroups revealed that NAXE downregulation occurred in the early stages of HCC, and was further decreased with development of HCC. This information indicated that early events leading to tumorigenesis may also contributed to NAXE downregulation and that its downregulation played an important role in promoting the progression of HCC, suggesting

that NAXE could be an ideal target for intervention for HCC treatment. Some other interesting phenomena attracted our attention too. First, NAXE expression in NHCC was significantly lower than in SLHCC and SHCC and our previous study had demonstrated that NHCC had the greatest metastatic potential among the 3 HCC subtypes.[18] Second, HCC cell lines with higher metastatic capacity had relative lower NAXE expression. Third, NAXE protein expression decreased progressively from ANLT, HCC tissue, to MVI, which is a well known predictor for HCC metastasis.[42] Fourth, low NAXE expression was associated with MVI and its combination with MVI predicted poorer prognosis of HCC patients. These results indicated that low NAXE expression may promote HCC invasive and metastasis. Indeed, our functional experiments confirmed that NAXE downregulation clearly promoted HCC migration and invasion in vitro, as well as progression in vivo. These results compelled us to explore the mechanisms by which NAXE downregulation promoted HCC progression.

Recently, accumulating evidence has indicated that EMT is associated with a cancer metastatic cascade.[26,43] Moreover, EMT could potentiate tumor angiogenesis and intravasation, thereby allowing the formation of MVI.[44,45] Intriguingly, we found that NAXE could

maintain the epithelial phenotype of HCC cells. We also revealed that low NAXE expression activated HIF-1α signaling even in aerobic environments and further facilitated HCC invasion, metastasis, and EMT. HIF-1α plays a critical role in tumor angiogenesis and metastasis by regulating multiple critical steps within angiogenesis and the metastatic cascade, including EMT processes.[32] Therefore, HIF-1α signaling activation resulting from NAXE downregulation in HCC could activate the EMT process and also stimulate angiogenesis, thereby combining to promote vascular invasion, which may be the molecular foundation of NAXE's discrimination ability for poor prognosis before the presence of vascular invasion. That is to say, early downregulation of NAXE may be a "marker" of MVI formation in the future.

Prolyl-hydroxylase-domain proteins (PHDs) could hydroxylate HIF-1a for degradation by the proteasome and require O_2, ferrous iron [Fe(II)] for full function. The downregulation of NAXE in HCC could lead to ROS accumulation, which could directly oxidate ferrous iron in PHDs. Oxidative PHDs cannot hydroxylate HIF-1a for degradation by the proteasome even in aerobic conditions.[46] Some studies have shown that loss-of-function of some genes could result in ROS elevation and further stabilize HIF-1α in normoxic conditions.[47,48] Therefore, NAXE downregulation in HCC could contribute to ROS accumulation and further PHD inactivation, which would finally lead to HIF-1a stabilization. In addition to HIF-1α, excess ROS could activate many signaling pathways associated with EMT of tumor cells, such as TP53, AP-1, NF-κB, HSF1, and so on. It is improbable that all these signaling are activated simultaneously and to what extent these signals is differentially activated by oxidative stress is uncertain.[49] Here, we found that just hypoxic signaling was altered by NAXE in HCC. Different signaling is likely to respond to distinct threshold levels of ROS concentration. In addition, subcellular compartment of oxidative stress could also affect the activation of redox signaling.[50] Mitochondria is a major source of ROS and there is crosstalk between HIF-1α and mitochondria.[51] Although more research is needed, we speculated that an appropriate ROS level caused by NAXE downregulation and its subcellular localization may jointly lead to the activation of hypoxic signaling. Previous studies have reported that NAC administration could inhibit tumor formation in a xenograft model.[52,53] In this study, we found that NAC administration in mouse drinking water significantly inhibited tumor growth and metastasis caused by NAXE downregulation. It means that, for HCC patients with low NAXE expression, NAC treatment would provide a promising avenue to inhibit HCC progression. Taken together, our study uncovered the suppressive role of NAXE in HCC and the clinical significance of NAXE may lie not only in its role for prediction of prognosis but also in its role for targeted therapy.

ORCID

Bo Sun https://orcid.org/0000-0002-7999-7071
Cong Xu https://orcid.org/0000-0002-9571-326X
Lian-Yue Yang https://orcid.org/0000-0002-8805-872X

REFERENCES

1. Bray F, Ferlay J, Soerjomataram I, Siegel RL, Torre LA, Jemal A. Global cancer statistics 2018: GLOBOCAN estimates of incidence and mortality worldwide for 36 cancers in 185 countries. *CA Cancer J Clin*. 2018;68:394-424.
2. Zhou M, Wang H, Zeng X, et al. Mortality, morbidity, and risk factors in China and its provinces, 1990–2017: a systematic analysis for the Global Burden of Disease Study 2017. *Lancet*. 2019;394:1145-1158.
3. Liu YC, Yeh CT, Lin KH. Cancer stem cell functions in hepatocellular carcinoma and comprehensive therapeutic strategies. *Cells*. 2020;9(6):1331.
4. Hanahan D, Weinberg RA. Hallmarks of cancer: the next generation. *Cell*. 2011;144:646-674.
5. Radisky DC, Levy DD, Littlepage LE, et al. Rac1b and reactive oxygen species mediate MMP-3-induced EMT and genomic instability. *Nature*. 2005;436:123-127.
6. Yun M, Choi AJ, Woo SR, et al. Inhibition of carbonyl reductase 1 enhances metastasis of head and neck squamous cell carcinoma through beta-catenin-mediated epithelial-mesenchymal transition. *J Cancer*. 2020;11:533-541.
7. Cairns RA, Harris IS, Mak TW. Regulation of cancer cell metabolism. *Nat Rev Cancer*. 2011;11:85-95.
8. Marbaix AY, Noel G, Detroux AM, Vertommen D, Van Schaftingen E, Linster CL. Extremely conserved ATP- or ADP-dependent enzymatic system for nicotinamide nucleotide repair. *J Biol Chem*. 2011;286:41246-41252.
9. Yoshida A, Dave V. Inhibition of NADP-dependent dehydrogenases by modified products of NADPH. *Arch Biochem Biophys*. 1975;169:298-303.
10. Spiegel R, Shaag A, Shalev S, Elpeleg O. Homozygous mutation in the APOA1BP is associated with a lethal infantile leukoencephalopathy. *Neurogenetics*. 2016;17:187-190.
11. Kremer LS, Danhauser K, Herebian D, et al. NAXE mutations disrupt the cellular NAD(P)HX repair system and cause a lethal neurometabolic disorder of early childhood. *Am J Hum Genet*. 2016;99:894-902.
12. Trinh J, Imhoff S, Dulovic-Mahlow M, et al. Novel NAXE variants as a cause for neurometabolic disorder: implications for treatment. *J Neurol*. 2020;267:770-782.
13. Marbaix AY, Tyteca D, Niehaus TD, Hanson AD, Linster CL, Van Schaftingen E. Occurrence and subcellular distribution of the NADPHX repair system in mammals. *Biochem J*. 2014;460:49-58.
14. Nathan C, Ding A. SnapShot: reactive oxygen intermediates (ROI). *Cell*. 2010;140:951.
15. Zhang T, Wang Q, Wang Y, et al. AIBP and APOA-I synergistically inhibit intestinal tumor growth and metastasis by promoting cholesterol efflux. *J Transl Med*. 2019;17:161.
16. Ritter M, Buechler C, Boettcher A, et al. Cloning and characterization of a novel apolipoprotein A-I binding protein, AI-BP, secreted by cells of the kidney proximal tubules in response to HDL or ApoA-I. *Genomics*. 2002;79:693-702.

17. Altman DG, McShane LM, Sauerbrei W, Taube SE. Reporting recommendations for tumor marker prognostic studies (REMARK): explanation and elaboration. *BMC Med.* 2012;10:51.

18. Yang LY, Fang F, Ou DP, Wu W, Zeng ZJ, Wu F. Solitary large hepatocellular carcinoma: a specific subtype of hepatocellular carcinoma with good outcome after hepatic resection. *Ann Surg.* 2009;249:118-123.

19. Wang W, Yang L-Y, Huang G-W, et al. Genomic analysis reveals RhoC as a potential marker in hepatocellular carcinoma with poor prognosis. *Br J Cancer.* 2004;90:2349-2355.

20. Yang LY, Wang W, Peng JX, Yang JQ, Huang GW. Differentially expressed genes between solitary large hepatocellular carcinoma and nodular hepatocellular carcinoma. *World J Gastroenterol.* 2004;10:3569-3573.

21. Tang Z-Y, Ye S-L, Liu Y-K, et al. A decade's studies on metastasis of hepatocellular carcinoma. *J Cancer Res Clin Oncol.* 2004;130:187-196.

22. Dou C-Y, Cao C-J, Wang Z, et al. EFEMP1 inhibits migration of hepatocellular carcinoma by regulating MMP2 and MMP9 via ERK1/2 activity. *Oncol Rep.* 2016;35:3489-3495.

23. Chung KY, Cheng IK, Ching AK, Chu JH, Lai PB, Wong N. Block of proliferation 1 (BOP1) plays an oncogenic role in hepatocellular carcinoma by promoting epithelial-to-mesenchymal transition. *Hepatology.* 2011;54:307-318.

24. Yang B, Feng X, Liu H, et al. High-metastatic cancer cells derived exosomal miR92a-3p promotes epithelial-mesenchymal transition and metastasis of low-metastatic cancer cells by regulating PTEN/Akt pathway in hepatocellular carcinoma. *Oncogene.* 2020;39:6529-6543.

25. Kulis M, Esteller M. DNA methylation and cancer. *Adv Genet.* 2010;70:27-56.

26. Nieto MA, Huang RY, Jackson RA, Thiery JP. EMT: 2016. *Cell.* 2016;166:21-45.

27. Yang J, Weinberg RA. Epithelial-mesenchymal transition: at the crossroads of development and tumor metastasis. *Dev Cell.* 2008;14:818-829.

28. Wilson GK, Tennant DA, McKeating JA. Hypoxia inducible factors in liver disease and hepatocellular carcinoma: current understanding and future directions. *J Hepatol.* 2014;61:1397-1406.

29. Semenza GL. Hypoxia-inducible factors in physiology and medicine. *Cell.* 2012;148:399-408.

30. Huang LE, Gu J, Schau M, Bunn HF. Regulation of hypoxia-inducible factor 1alpha is mediated by an O_2-dependent degradation domain via the ubiquitin-proteasome pathway. *Proc Natl Acad Sci USA.* 1998;95:7987-7992.

31. Guo Y, Xiao Z, Yang L, et al. Hypoxiainducible factors in hepatocellular carcinoma (Review). *Oncol Rep.* 2020;43:3-15.

32. Rankin EB, Giaccia AJ. Hypoxic control of metastasis. *Science.* 2016;352:175-180.

33. Keith B, Johnson RS, Simon MC. HIF1alpha and HIF2alpha: sibling rivalry in hypoxic tumour growth and progression. *Nat Rev Cancer.* 2011;12:9-22.

34. Gerald D, Berra E, Frapart YM, et al. JunD reduces tumor angiogenesis by protecting cells from oxidative stress. *Cell.* 2004;118:781-794.

35. Sullivan L, Martinez-Garcia E, Nguyen H, et al. The proto-oncometabolite fumarate binds glutathione to amplify ROS-dependent signaling. *Mol Cell.* 2013;51:236-248.

36. Gao P, Zhang H, Dinavahi R, et al. HIF-dependent antitumorigenic effect of antioxidants in vivo. *Cancer Cell.* 2007;12:230-238.

37. Fang L, Choi S-H, Baek JS, et al. Control of angiogenesis by AIBP-mediated cholesterol efflux. *Nature.* 2013;498:118-122.

38. Gu Q, Yang X, Lv J, et al. AIBP-mediated cholesterol efflux instructs hematopoietic stem and progenitor cell fate. *Science.* 2019;363:1085-1088.

39. Zhang M, Zhao G-J, Yao F, et al. AIBP reduces atherosclerosis by promoting reverse cholesterol transport and ameliorating inflammation in apoE(-/-) mice. *Atherosclerosis.* 2018;273:122-130.

40. Sorci-Thomas MG, Thomas MJ. AIBP, NAXE, and angiogenesis: what's in a name? *Circ Res.* 2017;120:1690-1691.

41. Navab M, Reddy ST, Van Lenten BJ, Fogelman AM. HDL and cardiovascular disease: atherogenic and atheroprotective mechanisms. *Nat Rev Cardiol.* 2011;8:222-232.

42. Rodriguez-Peralvarez M, Luong TV, Andreana L, Meyer T, Dhillon AP, Burroughs AK. A systematic review of microvascular invasion in hepatocellular carcinoma: diagnostic and prognostic variability. *Ann Surg Oncol.* 2013;20:325-339.

43. Giannelli G, Koudelkova P, Dituri F, Mikulits W. Role of epithelial to mesenchymal transition in hepatocellular carcinoma. *J Hepatol.* 2016;65:798-808.

44. Wang X, Ma C, Zong Z, et al. A20 inhibits the motility of HCC cells induced by TNF-alpha. *Oncotarget.* 2016;7:14742-14754.

45. Xu Z-Y, Ding S-M, Zhou L, et al. FOXC1 contributes to microvascular invasion in primary hepatocellular carcinoma via regulating epithelial-mesenchymal transition. *Int J Biol Sci.* 2012;8:1130-1141.

46. Pouyssegur J, Mechta-Grigoriou F. Redox regulation of the hypoxia-inducible factor. *Biol Chem.* 2006;387:1337-1346.

47. Guzy RD, Sharma B, Bell E, Chandel NS, Schumacker PT. Loss of the SdhB, but not the SdhA, subunit of complex II triggers reactive oxygen species-dependent hypoxia-inducible factor activation and tumorigenesis. *Mol Cell Biol.* 2008;28:718-731.

48. Horak P, Crawford AR, Vadysirisack DD, et al. Negative feedback control of HIF-1 through REDD1-regulated ROS suppresses tumorigenesis. *Proc Natl Acad Sci USA.* 2010;107:4675-4680.

49. Hayes JD, Dinkova-Kostova AT, Tew KD. Oxidative stress in cancer. *Cancer Cell.* 2020;38:167-197.

50. Hansen JM, Go YM, Jones DP. Nuclear and mitochondrial compartmentation of oxidative stress and redox signaling. *Annu Rev Pharmacol Toxicol.* 2006;46:215-234.

51. Fuhrmann DC, Brune B. Mitochondrial composition and function under the control of hypoxia. *Redox Biol.* 2017;12:208-215.

52. Bell EL, Emerling BM, Ricoult SJ, Guarente L. SirT3 suppresses hypoxia inducible factor 1alpha and tumor growth by inhibiting mitochondrial ROS production. *Oncogene.* 2011;30:2986-2996.

53. Anastasiou D, Poulogiannis G, Asara JM, et al. Inhibition of pyruvate kinase M2 by reactive oxygen species contributes to cellular antioxidant responses. *Science.* 2011;334:1278-1283.

SUPPORTING INFORMATION

Additional supporting information may be found online in the Supporting Information section.